

# Monte Carlo simulations in neutrino physics: the example of the SOX experiment

A. Caminata<sup>1</sup>, M. Agostini<sup>2</sup>, K. Altenmüller<sup>2</sup>, S. Appel<sup>2</sup>, G. Bellini<sup>3</sup>, J. Benziger<sup>4</sup>, N. Berton<sup>5</sup>, D. Bick<sup>6</sup>, G. Bonfini<sup>7</sup>, D. Bravo<sup>8</sup>, B. Caccianiga<sup>3</sup>, F. Calaprice<sup>9</sup>, M. Carlini<sup>7</sup>, P. Cavalcante<sup>7</sup>, A. Chepurinov<sup>10</sup>, K. Choi<sup>11</sup>, M. Cribier<sup>5</sup>, D. D'Angelo<sup>3</sup>, S. Davini<sup>12</sup>, A. Derbin<sup>13</sup>, L. Di Noto<sup>1</sup>, I. Drachnev<sup>12</sup>, M. Durero<sup>5</sup>, A. Etenko<sup>14</sup>, S. Farinon<sup>1</sup>, V. Fischer<sup>5</sup>, K. Fomenko<sup>15</sup>, A. Formozov<sup>3,15</sup>, D. Franco<sup>16</sup>, F. Gabriele<sup>7</sup>, J. Gaffiot<sup>5</sup>, C. Galbiati<sup>9</sup>, C. Ghiano<sup>1</sup>, M. Giammarchi<sup>3</sup>, M. Goeger-Neff<sup>2</sup>, A. Goretti<sup>9</sup>, M. Gromov<sup>10</sup>, C. Hagner<sup>6</sup>, Th. Houdy<sup>5</sup>, E. Hungerford<sup>17</sup>, Aldo Ianni<sup>7</sup>, Andrea Ianni<sup>9</sup>, N. Jonquères<sup>18</sup>, K. Jedrzejczak<sup>19</sup>, D. Jeschke<sup>2</sup>, M. Kaiser<sup>6</sup>, V. Kobychyev<sup>20</sup>, D. Korablev<sup>15</sup>, G. Korga<sup>7</sup>, V. Kornoukhov<sup>21</sup>, D. Kryn<sup>16</sup>, T. Lachenmaier<sup>22</sup>, T. Lasserre<sup>5</sup>, M. Laubenstein<sup>7</sup>, B. Lehnert<sup>23</sup>, J. Link<sup>8</sup>, E. Litvinovich<sup>14,24</sup>, F. Lombardi<sup>7</sup>, P. Lombardi<sup>3</sup>, L. Ludhova<sup>3</sup>, G. Lukyanchenko<sup>14,24</sup>, I. Machulin<sup>14,24</sup>, S. Manecki<sup>8</sup>, W. Maneschg<sup>28</sup>, S. Marcocci<sup>12</sup>, J. Maricic<sup>11</sup>, G. Mention<sup>5</sup>, E. Meroni<sup>3</sup>, M. Meyer<sup>6</sup>, L. Miramonti<sup>3</sup>, M. Misiaszek<sup>7,19</sup>, M. Montuschi<sup>25</sup>, P. Mosteiro<sup>9</sup>, V. Muratova<sup>13</sup>, R. Musenich<sup>1</sup>, B. Neumair<sup>2</sup>, L. Oberauer<sup>2</sup>, M. Obolensky<sup>16</sup>, F. Ortica<sup>26</sup>, M. Pallavicini<sup>1</sup>, L. Papp<sup>2</sup>, L. Perasso<sup>1</sup>, A. Pocar<sup>27</sup>, G. Ranucci<sup>3</sup>, A. Razeto<sup>7</sup>, A. Re<sup>3</sup>, A. Romani<sup>26</sup>, R. Roncin<sup>7,16</sup>, N. Rossi<sup>7</sup>, S. Schönert<sup>2</sup>, L. Scola<sup>5</sup>, D. Semenov<sup>13</sup>, H. Singen<sup>28</sup>, M. Skorokhvatov<sup>14,24</sup>, O. Smirnov<sup>15</sup>, A. Sotnikov<sup>15</sup>, S. Sukhotin<sup>13</sup>, Y. Suvorov<sup>14,29</sup>, R. Tartaglia<sup>7</sup>, G. Testera<sup>1</sup>, J. Thurn<sup>23</sup>, M. Toropova<sup>14</sup>, C. Veyssière<sup>5</sup>, M. Vivier<sup>5</sup>, E. Unzhakov<sup>13</sup>, R.B. Vogelaar<sup>8</sup>, F. von Feilitzsch<sup>2</sup>, H. Wang<sup>29</sup>, S. Weinz<sup>30</sup>, J. Winter<sup>30</sup>, M. Wojcik<sup>19</sup>, M. Wurm<sup>30</sup>, Z. Yokley<sup>8</sup>, O. Zaimidoroga<sup>15</sup>, S. Zavatarelli<sup>1</sup>, K. Zuber<sup>23</sup>, G. Zuzel<sup>19</sup>

<sup>1</sup>Dipartimento di Fisica, Università degli Studi e INFN, Genova 16146, Italy

<sup>2</sup>Physik-Department and Excellence Cluster Universe, Technische Universität München, 85748 Garching, Germany

<sup>3</sup>Dipartimento di Fisica, Università degli Studi e INFN, 20133 Milano, Italy

<sup>4</sup>Chemical Engineering Department, Princeton University, Princeton, NJ 08544, USA

<sup>5</sup>Commisariat à l'Énergie Atomique et aux Énergies Alternatives, Centre de Saclay, IRFU, 91191 Gif-sur-Yvette, France

<sup>6</sup>Institut für Experimentalphysik, Universität Hamburg, 22761 Hamburg, Germany

<sup>7</sup>INFN Laboratori Nazionali del Gran Sasso, 67010 Assergi (AQ), Italy

<sup>8</sup>Physics Department, Virginia Polytechnic Institute and State University, Blacksburg, VA 24061, USA

<sup>9</sup>Physics Department, Princeton University, Princeton, NJ 08544, USA

<sup>10</sup>Lomonosov Moscow State University Skobeltsyn Institute of Nuclear Physics, 119234 Moscow, Russia

<sup>11</sup>Department of Physics and Astronomy, University of Hawai'i, Honolulu, HI 96822, USA

<sup>12</sup>Gran Sasso Science Institute (INFN), 67100 L'Aquila, Italy

<sup>13</sup>St. Petersburg Nuclear Physics Institute NRC Kurchatov Institute, 188350 Gatchina, Russia

<sup>14</sup>NRC Kurchatov Institute, 123182 Moscow, Russia

<sup>15</sup>Joint Institute for Nuclear Research, 141980 Dubna, Russia

<sup>16</sup>AstroParticule et Cosmologie, Universit Paris Diderot, CNRS/IN2P3, CEA/IRFU, Observatoire de Paris, Sorbonne Paris Cit, 75205 Paris Cedex 13, France

<sup>17</sup>Department of Physics, University of Houston, Houston, TX 77204, USA

<sup>18</sup>Commissariat à l'Énergie Atomique et aux Énergies Alternatives, Centre de Saclay, DEN/DM2S/SEMT/BCCR, 91191 Gif-sur-Yvette, France

<sup>19</sup>M. Smoluchowski Institute of Physics, Jagiellonian University, 30059 Krakow, Poland

<sup>20</sup>Kiev Institute for Nuclear Research, 06380 Kiev, Ukraine

<sup>21</sup>Institute for Theoretical and Experimental Physics, 117218 Moscow, Russia

<sup>22</sup>Kepler Center for Astro and Particle Physics, Universität Tübingen, 72076 Tübingen, Germany

<sup>23</sup>Department of Physics, Technische Universität Dresden, 01062 Dresden, Germany

<sup>24</sup>National Research Nuclear University MEPhI (Moscow Engineering Physics Institute), 115409 Moscow, Russia

<sup>25</sup>Dipartimento di Fisica e Scienze della Terra Università degli Studi di Ferrara e INFN, Via Saragat 1-44122, Ferrara, Italy

<sup>26</sup>Dipartimento di Chimica, Università e INFN, 06123 Perugia, Italy

<sup>27</sup>Amherst Center for Fundamental Interactions and Physics Department, University of Massachusetts, Amherst, MA 01003, USA

<sup>28</sup>Max-Planck-Institut für Kernphysik, 69117 Heidelberg, Germany

<sup>29</sup>Physics and Astronomy Department, University of California Los Angeles (UCLA), Los Angeles, California 90095, USA

<sup>30</sup>Institute of Physics and Excellence Cluster PRISMA, Johannes Gutenberg-Universität Mainz, 55099 Mainz, Germany

**DOI:** <http://dx.doi.org/10.3204/DESY-PROC-2016-05/21>

The SOX project aims to test the existence of light sterile neutrinos. A solid signal would mean the discovery of the first particles beyond the Standard Electroweak Model and would have profound implications in our understanding of the Universe and of fundamental particle physics. In case of a negative result, it is able to close a long standing debate about the reality of the neutrino anomalies. The SOX experiment will use a  $^{144}\text{Ce}$ - $^{144}\text{Pr}$  antineutrino generator placed at short distance from the Borexino liquid scintillator detector. Particular emphasis is devoted in describing how a simulation of a neutrino detector is implemented and how it can be used to obtain useful information for the future data analysis.

## 1 Introduction

Although most of the collected neutrino experimental data in neutrino flux rates and their oscillations fit well into the three-flavour oscillation model, several short-baseline neutrino experiments have reported anomalies which significantly deviates from the three active neutrino pictures ([1, 2, 3, 4]).

All these anomalies can be related to the presence of a forth type of neutrino with  $\Delta m_{14}^2$  of about  $1 \text{ eV}^2$ . This new particle, not predicted from the standard model, is called sterile since it is not coupled with the  $Z^0$  boson. The SOX project will exploit the unprecedented performances of the Borexino detector to investigate the existence of unexpected oscillations in the low  $L/E$  region and therefore investigate the existence of sterile neutrinos in the  $\Delta m_{14}^2$

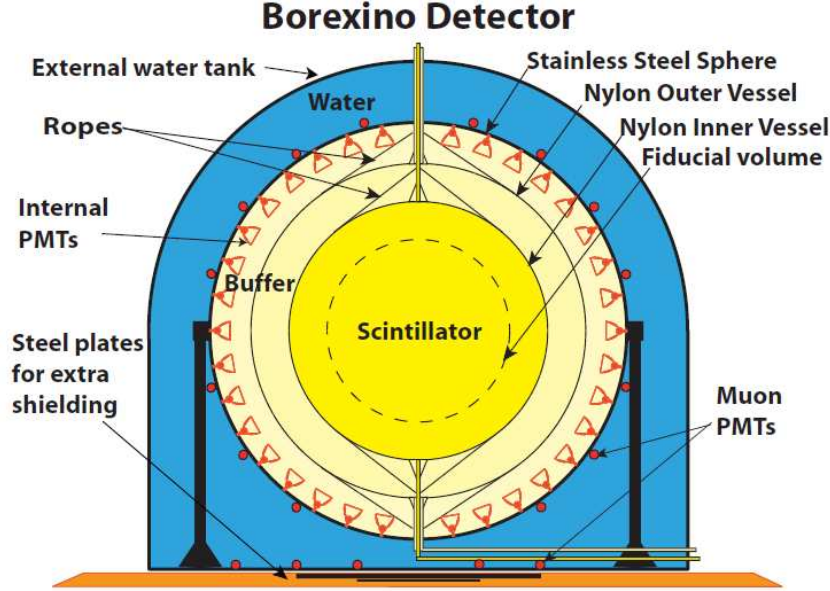


Figure 1: Schematic drawing of the Borexino detector.

region of  $\sim 1 \text{ eV}^2$  [5]. The first part of the project consists in deploying a 150 kCi  $^{144}\text{Ce} - ^{144}\text{Pr}$   $\bar{\nu}_e$  source in a dedicated pit located 8.5 m below the detector's center.

## 2 Antineutrino detection in Borexino

### 2.1 The Borexino detector

Borexino is an underground liquid scintillator detector located at Laboratori Nazionali del Gran Sasso in Italy [6]. It has an active mass of 278 tons of pseudocumene (PC, 1,2,4-trimethylbenzene), doped with 1.5 g/liter of PPO (2,5-diphenyloxazole, a fluorescent dye). The scintillator is contained in a thin nylon vessel (125  $\mu\text{m}$  in thickness) and it is surrounded by two concentric PC buffers doped with 2 g/liter of DMP (dimethylphthalate), a component that quenches the PC scintillation light. The two PC buffers are separated by a second thin nylon membrane to prevent radon diffusion toward the scintillator. The scintillator and buffers are contained in a stainless steel sphere (SSS) with diameter of 13.7 m. The scintillation light is detected by 2212 8 inch PMTs uniformly distributed in the inner surface of the SSS. The detector energy and vertex reconstruction performances are respectively 5% at 1 MeV and 15 cm. Antineutrinos are detected in Borexino by means of inverse beta decay (IBD, 1.8 MeV threshold) on protons. IBD events are clearly tagged using the space-time coincidence between the prompt  $e^+$  signal and the delayed neutron capture ( $\tau = 254 \mu\text{s}$  [7]) event. Therefore, accidental background is almost negligible. A 18.0-m diameter - 16.9-m high domed water tank

(WT) containing 2100 tons of ultrapure water surrounds the SSS providing additional shielding against external background. Moreover, additional 208 8-inch PMTs instrument the WT and detect the Cherenkov light radiated by muons in the water shield, serving as muon veto. Right beneath the Borexino detector, there is a cubical pit (side 105 cm) accessible through a small squared tunnel (side 95 cm) that was built at the time of construction with the purpose of housing possible neutrino sources. The existence of this tunnel is one of the reasons why the  $^{144}\text{Ce}$  source can be deployed with no changes to the Borexino layout. The center of the pit is at 8.5 m from the detector center, requiring a relatively high source activity for the source.

## 2.2 The antineutrino source

The antineutrino source must accomplish to several requirements. To get a reasonable number of interaction inside the active volume, an activity of about 100 kCi is required. Moreover, since antineutrinos are detected via inverse beta decay (IBD), an energy spectrum that extends above the IBD threshold is necessary. Furthermore, the half-life must be reasonably long to produce and transport the source nearby the detector. The  $^{144}\text{Ce}$  source  $\beta$ -decays to  $^{144}\text{Pr}$  ( $t_{1/2} = 296$  days) which rapidly ( $t_{1/2} = 17$  min)  $\beta$ -decays to  $^{144}\text{Nd}$  emitting a spectrum of  $\bar{\nu}_e$  part of which falls above the IBD threshold (the endpoint of the  $^{144}\text{Pr}$  decay is about 3 MeV). The  $^{144}\text{Ce} - ^{144}\text{Pr}$  source has been identified as a suitable  $\bar{\nu}_e$  emitter having a long enough half-life to allow the source production and the transportation to LNGS.

The production of the source can be realized by isolating and extracting  $^{144}\text{Ce}$  from spent nuclear fuel (SNF). The source is produced as few kilograms of  $\text{CeO}_2$  containing a few tens of grams of  $^{144}\text{Ce}$ . The source emits also gamma rays that have to be shielded both for biological protection purposes and to avoid source-induced background. Consequently a cylindrical tungsten alloy shielding (density greater than  $18 \text{ g/cm}^3$ ) surrounds the source (which is contained in a stainless steel capsule). The shielding, 60 cm in height and diameter, has been designed driven by the 2.185 MeV gamma ray emitted with 0.7% intensity. Such dimensions ensure a 19-cm thick shielding and a  $10^{12}$  gamma-ray attenuation factor along any directions.

## 3 Data analysis

Borexino can study short distance neutrino oscillations in two ways. The first way is the standard disappearance technique (rate technique): if oscillations into sterile neutrino occur, the total count rate in the detector is lower than the expected rate without oscillations. Knowing the source activity (section 3.1) and measuring the interaction rate, it is possible to investigate the existence of the sterile neutrino state. The second way is based on an oscillometry measurement within the detector volume (shape technique).

If the values of  $m_{14}^2$  are of the order of  $1\text{eV}^2$  and the antineutrino energy is of the order of 1 MeV, the typical oscillation length is about a few meters, being smaller than the detector typical dimension and greater than the spatial resolution. Consequently, the resulting oscillations waves can be directly seen in Borexino and a direct measurement of  $m_{14}^2$  and  $\theta_{14}$  can be performed (figure 2). Figure 3 shows the best fit values for the current allowed phase space. Consequently, from the plot it is clear that the SOX experiment will investigate almost all the region of the neutrino anomaly.

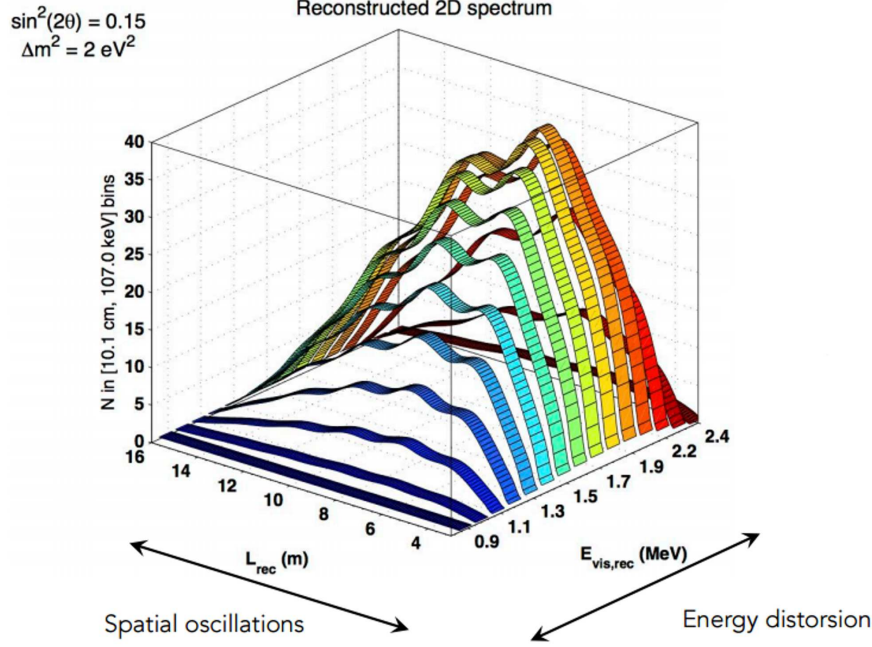


Figure 2: Oscillometry: waves in the reconstructed 2D spectrum for  $m_{14}^2 = 2\text{eV}^2$  and  $\sin^2(2\theta_{14}) = 0.15$ .

### 3.1 Calorimetric measurement

In case of rate analysis, it is fundamental to have a precise measurement (uncertainties below 1%) of the source activity. In order to infer the source activity, the heat released by the source is measured by two calorimeters (INFN-TUM and CEA). Both the calorimeters have been conceived to measure the source activity with high precision by knowing the power released by the radiation in the tungsten shield and absorbed by a water flow. In the INFN-TUM calorimeter, the water flows inside a copper heat exchanger in contact with the tungsten shield [8], while in the CEA calorimeter, the source with the tungsten is directly immersed in the water contained in the calorimeter apparatus. In both systems, neglecting the heat losses (that are measured by a calibration apparatus), the power is measured from the difference between the water temperature entering and exiting from the calorimeter and from the water mass flow.

## 4 Monte Carlo simulation code and the physics modelling the detector response

In order to properly take into account efficiencies and signal properties, for both the rate and shape analyses, a deep understanding of the detector behavior is necessary. Consequently, a full Monte Carlo simulation code has been developed.

Particles depositing energy in the scintillator produce light (both scintillation and Cherenkov

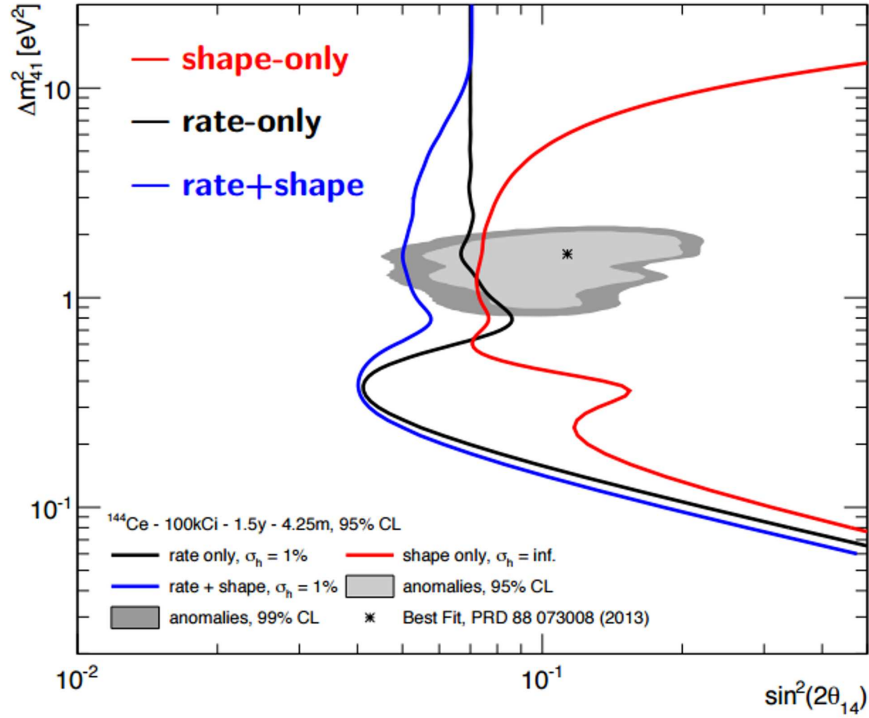


Figure 3: Neutrino anomaly region and foreseen sensitivity for SOX.

effect) which propagates inside the detector and it is detected by the 2212 PMTs. For each event, it is important to relate measurable quantities (the number of photons measured and the charge collected by each PMT, the time of arrival of each photon) with physical properties of the event (energy, position, particle identification). Consequently, a precise knowledge of the detector response for different particle types and energies is important for properly connecting measurable and physical quantities. The method of evaluation of the detector response function is based on a Monte Carlo simulation. This code is able to predict the shapes of the signal and the background both for SOX and solar neutrino analysis. The simulation takes into account all the processes that can influence the energy deposits inside the detector. The scintillation and Cherenkov light emission, the light propagation and detection processes are fully simulated. Moreover the read-out electronics is simulated as well. The Monte Carlo simulation output is a raw data file with the same format of the real data raw file, allowing an identical data processing. The simulation of the whole detector, from the energy deposit up to the detection of light is simulated using the standard GEANT4 [9] package. The simulation of the readout electronics is performed with a custom c++ code. In view of the Borexino phase II solar neutrino analysis and the SOX measurement, the Monte Carlo code has been extended. Particular attention has been devoted in developing generators for sterile neutrino signal as well as in improving the reliability of the light collection and the detector's response for events far away from the center. The code has been widely used for solar neutrino analysis and has been tested and validated deploying calibration sources inside the active volume and comparing the simulation



result with the acquired data (an example is reported in figure 4).

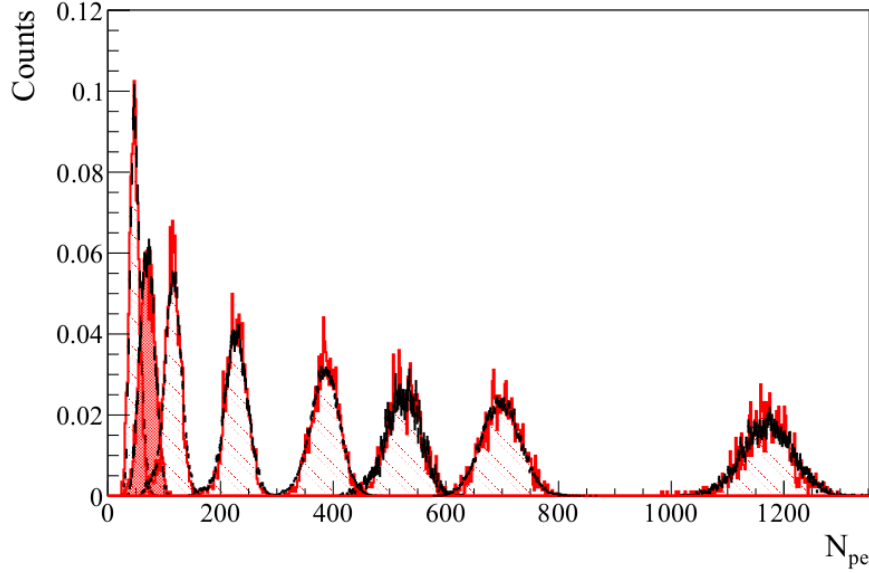


Figure 4: Comparison between data and Monte Carlo: several radioactive gamma sources have been deployed in the scintillator. In black the collected charge for real events, in red for simulated events. The agreement is better than 1%.

## 5 Conclusions

The Borexino detector is an ideal tool to search for sterile neutrinos. It is possible to test the existence of sterile neutrinos using an anti-neutrino source with almost negligible background. A deep knowledge of the detector response is fundamental for a proper interpretation of the acquired data. Consequently a Borexino Monte Carlo simulation code has been developed. In the last years the code has been refined and extended to take into account the SOX needs. Calibration campaigns with radioactive sources have been performed over the years. A new calibration is foreseen for the end of this year allowing a final tuning of the code before the start of the data-taking expected for the first part of 2017.

## References

- [1] Aguilar A *et al.* 2001 *Phys. Rev. D* **64** 112007
- [2] Aguilar A *et al.* 2013 *Phys. Rev. Lett.* **110** 161801
- [3] Mention G *et al.* 2011 *Phys. Rev. D* **83** 073006
- [4] Giunti C and Laveder M 2011 *Phys. Rev. C* **83** 065504
- [5] Bellini G *et al.* 2013 *JHEP* **38** 1308
- [6] Bellini G *et al.* 2014 *Phys. Rev. D* **89** 112007
- [7] Agostini M *et al.* 2015 *Phys. Rev. D* **92** 031101

- [8] Farninon S *et al.* 2016 *INFN technical note INFN-16-08/GE*
- [9] Geant4 Collaboration, Physics Reference Manual